Sensitivity of Arctic surface boundary layer process to sea ice concentrations: WRF atmospheric modeling study

Hyodae Seo (hseo@whoi.edu) and Jiayan Yang (jyang@whoi.edu), Physical Oceanography Department, Woods Hole Oceanographic Institution

The funds to support this research have been provided by ***The James M. and Ruth P. Clark Arctic Research Initiative*** fund.

1. Summary

Motivation and Goal: Sea ice concentration (SIC) is one of the most important factors influencing energy budget of the coupled boundary layer process in the Arctic. Currently, there are a number of satellite-based SIC datasets employing different retrieval algorithms, resulting in at times large regional discrepancy in SIC estimate. Goal of this study is to quantify the extent to which the Arctic atmosphere is sensitive to SIC estimates based on the Weather Forecast and Research (WRF) regional atmospheric model.

Method: We have carried out a series of one-month-long WRF integrations forced with four commonly used satellite-based SIC datasets, 1) NASA Team (NT), 2) Bootstrap (BT), 3) EUMETSAT Reprocessed sea ice (EUMET), and 4) Sea ice from NOAAOI SST (NOAA). The results are first verified against the in situ meteorological measurements at the Ice Station SHEBA (SHEBA) in winter (January) and summer (August) in 1998, and then at the Barrow Observatory (BRW).

Sea Ice Concentration (SIC): In winter, all four sea ice datasets agree well at the SHEBA site with ~1 SIC, while in summer, BT has consistently higher sea ice (0.95) than NT and NOAA (0.7) and EUMET (0.75). Disagreement in SIC tends to be pronounced in the marginal ice zone.

Model Performance: The model produces a reasonable agreement with the SHEBA measurements in terms of correlation and mean bias. In general, high correlations (>0.8) can be seen in dynamics fields (e.g., SLP), lower correlations (0.6-0.8) in thermodynamic fields (e.g., T2, Q2) and the lowest correlation (<0.6) in turbulent heat and longwave radiation flux. In winter, mean bias in SLP is +3hPa with the lower T2 and SKT of ~-1.5K. In summer, downward and upward shortwave radiation (SWd and SWu) show a mean bias of ~-6W/m^2 with a large inter-model spread. In winter, the downward longwave radiation (LWd) shows mean bias of -20 W/m^2 across all runs with minimal inter-model spread. WRF underestimates the liquid water path (LWP), indicative of less cloud in the atmosphere and hence less LWd.

Model Sensitivity at SHEBA: The largest uncertainty in mean field is found in SWd and SWu in summer, where the run with BT SIC produces higher SWd (>+20 W/m^2) and SWu (>+40 W/m^2) than three other runs.

Impact on Arctic Ocean: Simulated net heat (Qnet) and momentum flux (τ) linearly vary with SIC. Over the entire Arctic, the linear regression coefficients are larger in winter (27 W/m^2 per 0.1 variation in SIC) than in summer (~-8 W/m^2). Considering the range of SIC variation of each dataset and the mean Qnet (Table 1), this indicates that mean Qnet can vary by 55% in January and 45% in August depending on the chosen SIC datasets in WRF. Mean wind stress varies ~10% due to SIC.

Implication and Future Direction: This considerable sensitivity of meteorological fields and surface flux to the chosen SIC datasets implies that surface forcing fields can be an important source of simulation uncertainty in modeling of the Arctic Ocean. A more quantitative assessment of sensitivity to SIC should be made, along with an attempt to reduce the bias present in cloudiness and land-surface process. Multi-decadal simulation is underway using the Polar WRF v3.4.1 (Bromwich et al. 2009) to assess climatic impacts of SIC in Arctic.

2. Model, experiment, and data

Model: Weather Research and Forecast (WRF) 3.4 (Skamarock et al., 2008)
25 km horizontal resolution, 28 vertical layers (10 below 700 m).
Cloud Microphysics: WRF Single-Moment 6-class scheme,
Cumulus Convection: Grell-Devenyi (GD) ensemble scheme,
Land surface: Noah land surface model,
Planetary Boundary Layer: Mellor-Yamada-Janjic scheme

Experiment: *A series of 48-hour forecasts*
Downscaling for January and August 1998 in a forecast mode. Simulations consist of a series of 48-hour integrations initialized daily at 0000 UTC from the 1st day to the end of the month. The initial 24 hours as model spin-up time are disregarded and the model output with hour 25-48 hour is combined into month-long time-series. WRF run in "climate mode", with a single initialization beginning of the month and continuous integration, produces less skillful, but qualitatively similar results.

Initial and lateral boundary, and SST conditions
6-hourly ECMWF-Interim atmospheric reanalysis (Dee et al. 2011)

Sea Ice Concentration Datasets
1) **NT**: NASA Team algorithm Sea Ice Concentrations from Nimbus-7 SMMR, DMSP, SSM/I-SSMIS, daily 25 km (Cavalieri et al. 1996), http://nsidc.org/data/docs/daac/nsidc0051_gsfc_seaice.gd.html

2) **BT**: Bootstrap Sea Ice Concentrations from Nimbus-7 SMMR and DMSP SSM/I-SSMIS, daily 25 km (Comiso 2000), http://nsidc.org/data/nsidc-0079.html

3) **EUMET**: EUMETSAT Ocean and Sea Ice Satellite Application Facility (OSI SAF) Sea Ice Concentrations from Nimbus-7 SMMR and DMSP SSM/I-SSMIS, daily 6km, (Tonboe et al. 2011) http://nsidc.org/api/metadata?id=nsidc-0508

4) **NOAA**: NOAA OI.v2 (Reynolds et al. 2007) uses real-time sea ice concentrations generated from microwave satellite data by Grumbine (1996) with delayed sea ice concentrations by Cavalieri et al. (1999), daily 25 km, http://www.ncdc.noaa.gov/oa/climate/research/sst/oi-daily-information.php

Data for model validation
1. Ice Station SHEBA: http://www.eol.ucar.edu/projects/sheba/
2. Barrow Alaska Observatory:
http://www.esrl.noaa.gov/gmd/obop/brw/summary.html

3. Sea Ice concentrations in 4 datasets

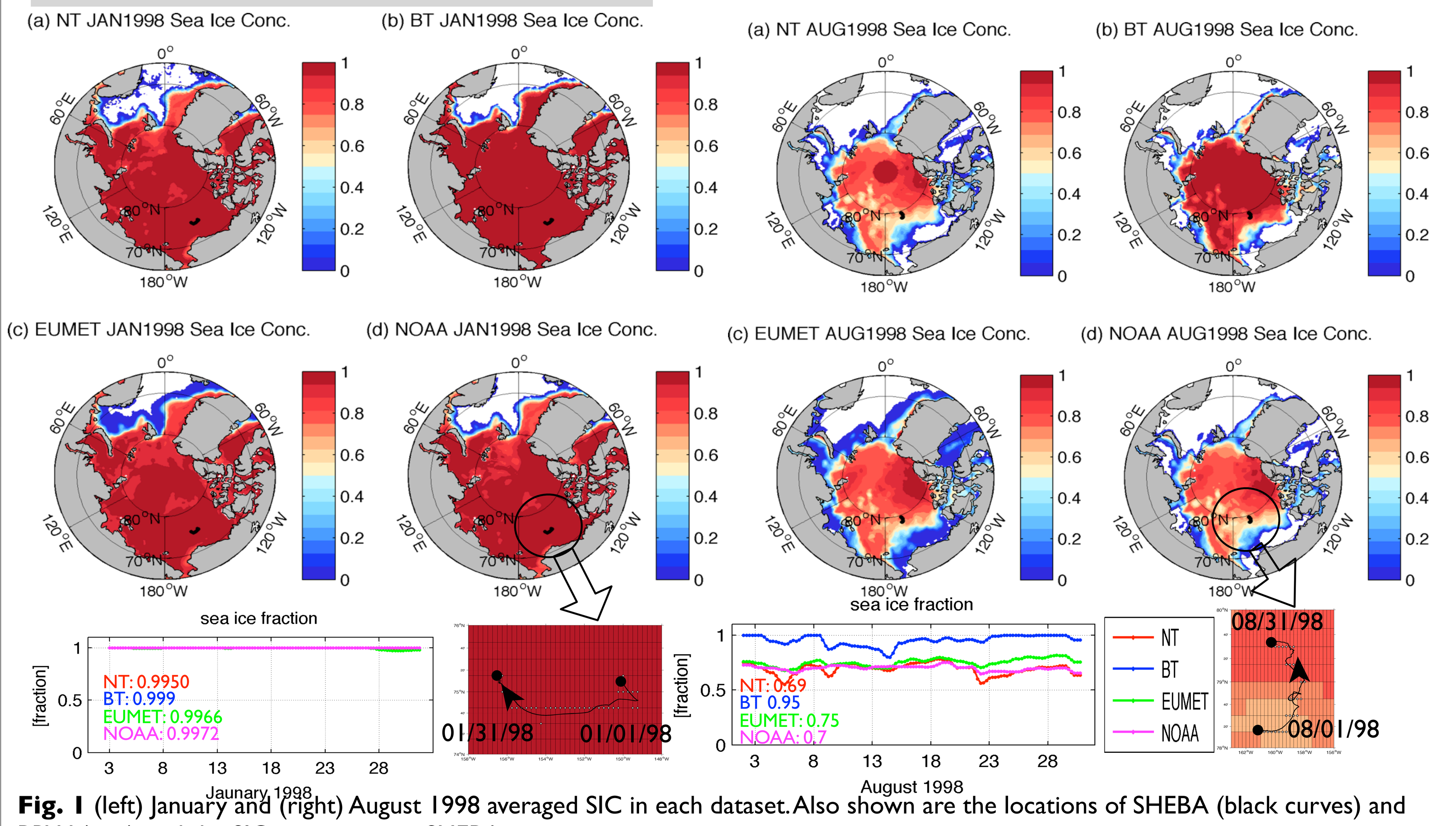

Fig. 1 (left) January and (right) August 1998 averaged SIC in each dataset. Also shown are the locations of SHEBA (black curves) and BRW (star), and the SIC time-series at SHEBA.

4. Validation at the Ice Station SHEBA

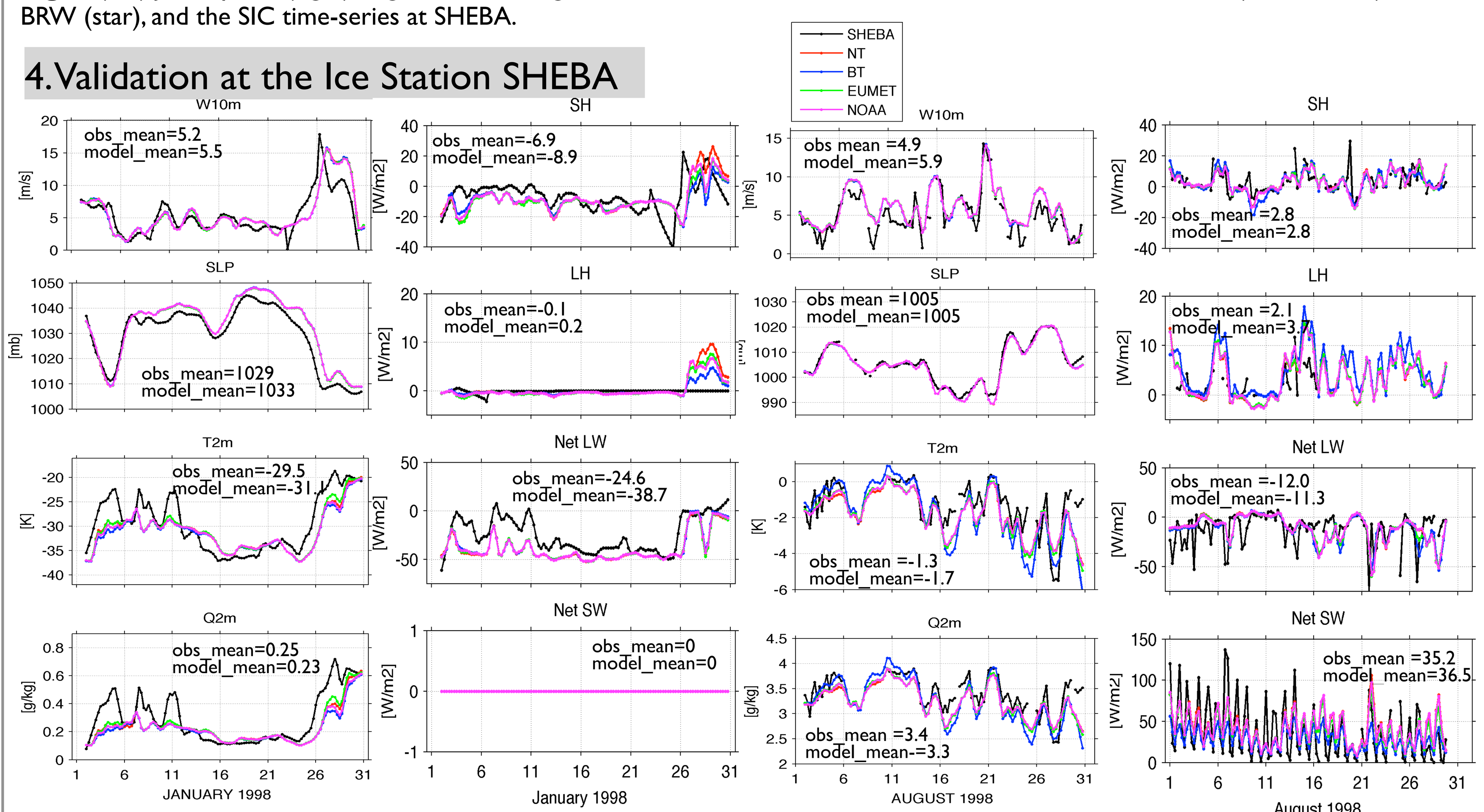

Fig. 2 Time-series of the met. variables and surface flux in January (left) and August (right) against the SHEBA observations.

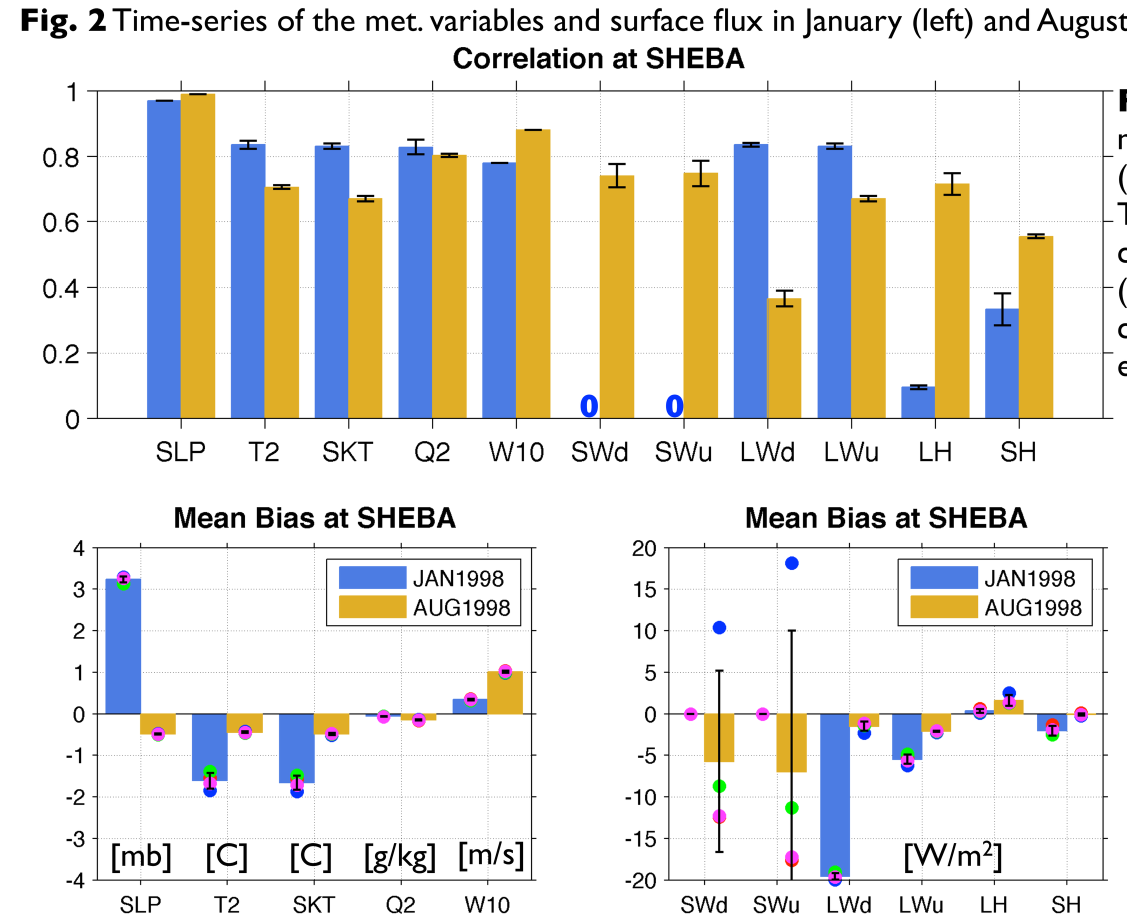

Fig. 3 (top) Correlation coefficients between the measurements at SHEBA Ice Station and model (averaged) for (blue) January and (yellow) August. The errorbars represent ±1 standard deviation of correlation coefficients from individual runs. (bottom) Mean bias (WRF-SHEBA) with colored circles denoting mean values in 4 individual runs. The error bars represent ±1 standard deviation in bias.

● NT ● BT ● EUMET ● NOAA

Both SWd and SWu show large sensitivity to SIC in summer, with the difference up to 40W/m^2 between BT and other three runs. This contributes to the large discrepancy in Qnet (Fig. 6) in Arctic Ocean.

4 WRF runs show large LWd bias (-20 W/m^2), indicating that this is not so much related to SIC, but maybe more has to with errors in model's representation of cloud micro-physics in winter. (Next figure).

5. Errors in Liquid/Ice Water Path

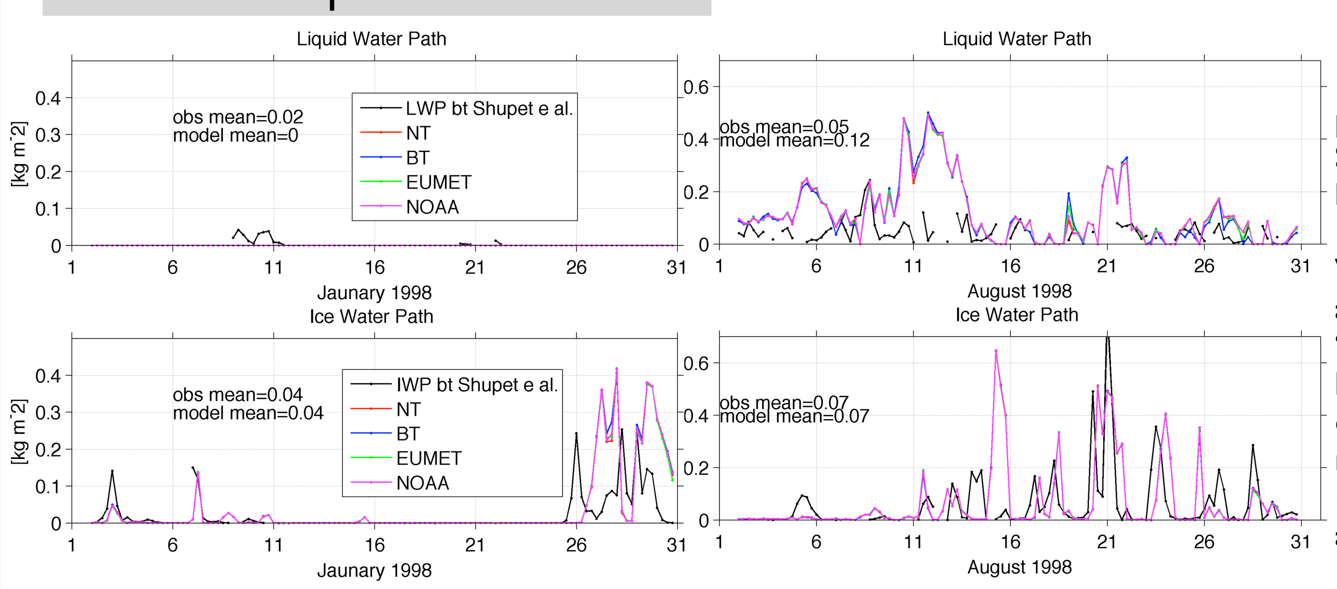

Fig. 4 Time-series of WRF liquid water path (LWP) and ice water path (IWP) at SHEBA site in comparison to retrievals by Shupe et al. (2005).

WRF LWP is nearly zero in January in all model runs. The limited "observations" indicate the presence of liquid cloud at SHEBA site. This discrepancy could partially cause the negative bias in LWdLWd in all model runs (Prenni et al. 2007, Bromwich et al. 2009).

6. Validation at the Barrow Observatory

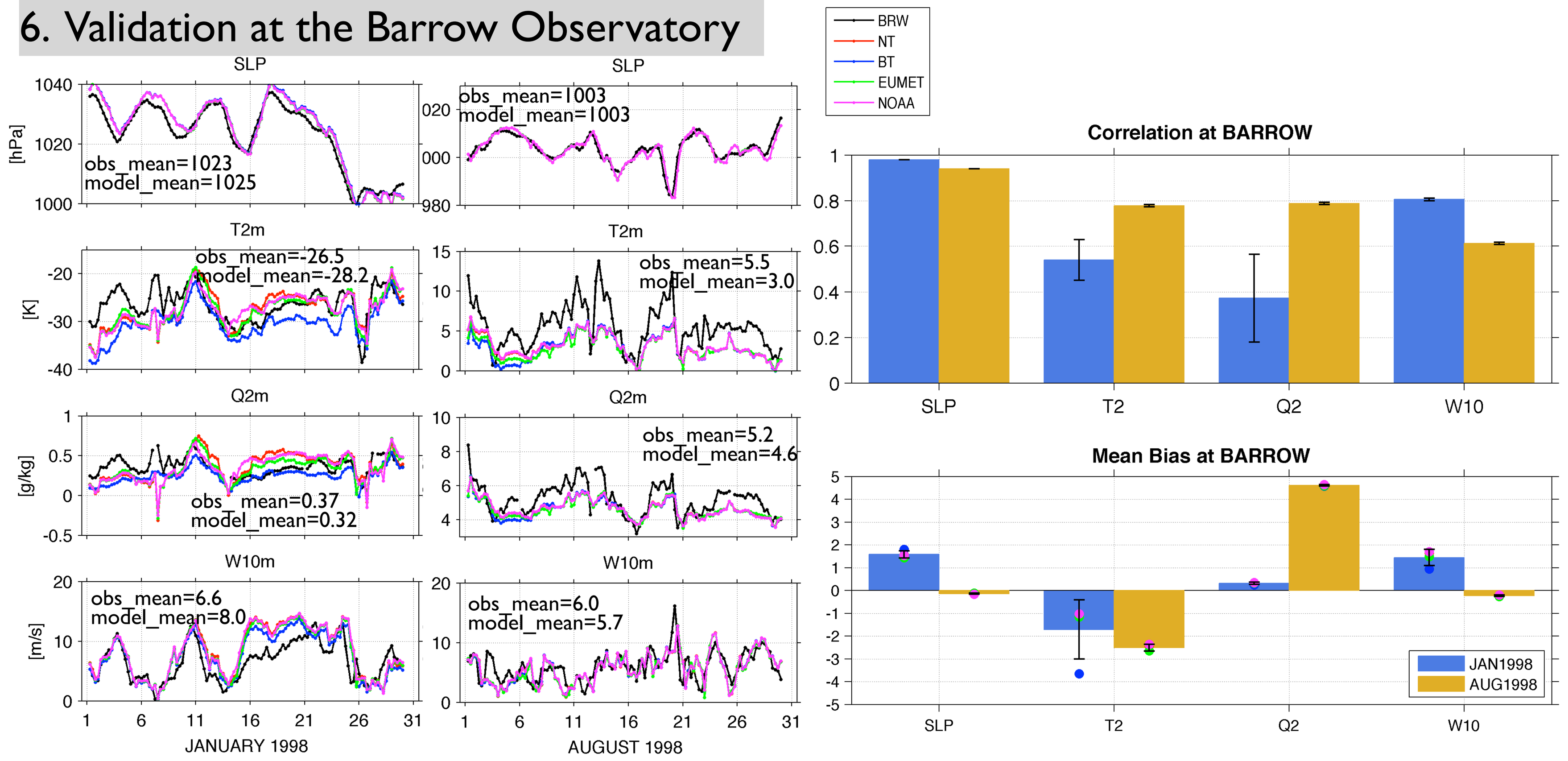

Fig. 5 (left) Time-series in SLP, T2, Q2, and W10 at BRW and model runs. (Right) Bar plots showing (top) correlation between the simulated and observed quantities, and (bottom) mean bias in winter (blue) and summer (yellow).

7. Sensitivity of heat and momentum flux to sea ice concentrations

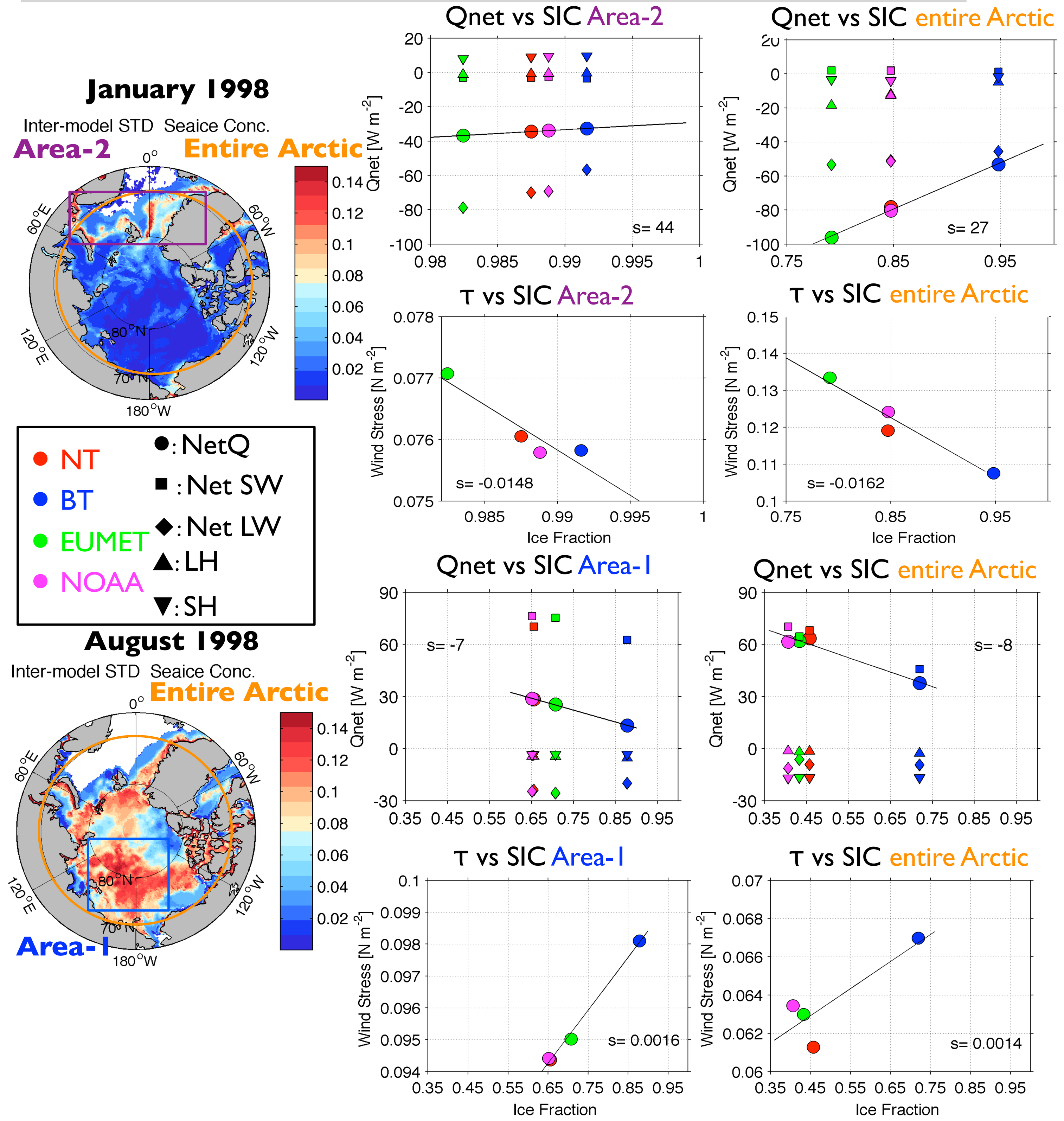

Fig. 6 (Left) Standard deviation of SIC in 4 datasets in color. (Right), scatter plots of SIC vs net heat flux (Qnet) and wind stress magnitude (τ). For Qnet, additional symbols denote each component of heat flux. s in each panel denotes the slope of linear fit (black line), with the unit of W/m^2 and N/m^2 per discrepancy SIC by 0.1.

		Qnet (W/m^2)			τ (N/m^2)		
		Mean	Max difference	(Max diff) / (Mean)	Mean	Max difference	(Max diff) / (Mean)
Winter	Area-2	-112	67	59%	0.142	0.031	22%
	Entire Arctic	-77	43	55%	0.212	0.026	12%
Summer	Area-1	24	15	62%	0.096	0.004	4%
	Entire Arctic	56	26	45%	0.064	0.006	10%

Table 1. Area-averaged net heat flux (Qnet) and wind stress magnitude (τ) showing mean value from 4 WRF runs, the maximum difference in model runs, and the percentage of difference to the mean.

Acknowledgement: HS thanks A. Proshutinsky for helpful comments and discussion.

References

Bromwich, et al. 2009: Development and Testing of Polar Weather Research and Forecasting Model: 2. Arctic Ocean. *JGR*, 114, D08122
Cavalieri, et al. 1996, updated yearly. Sea Ice Concentrations from Nimbus-7 SMMR and DMSP SSM/I-SSMIS Passive Microwave Data. Boulder, Co, USA: NSIDC.
Comiso. 2000, updated 2012. Bootstrap Sea Ice Concentrations from Nimbus-7 SMMR and DMSP SSM/I-SSMIS. Version 2.0. Boulder, Co, USA: NSIDC.
Dee et al., 2011: The ERA-Interim reanalysis: configuration and performance of the data assimilation system. QJRMS, 137, 553-597.
Reynolds et al. 2007: Daily High-Resolution-Blended Analyses for Sea Surface Temperature, . J. Climate, 20, 5473-5469
Prenni et al. 2007: Can ice-nucleating aerosols affect Arctic seasonal climate?, Bull. Am. Meteorol. Soc., 88, 541 – 550
Skamarock et al. 2008: A description of the advanced research WRF version 3. Rep. NCAR/TN-475+STR, NCAR, Boulder, Co.
Shupe et al. 2005: Cloud radiative forcing of the Arctic surface: The influence of clouds properties, surface albedo, and solar zenith angle, J. Clim., 17, 616–628
Tonboe, et al 2011. EUMETSAT OSI SAF Global Sea Ice Concentration Reprocessing Data. Boulder, Co, USA: NSIDC.